SLAC – PUB – 3892
February 1986
(A)

SOME ISSUES INVOLVED IN DESIGNING A 1 TeV (c.m.) $e^{\pm}$ LINEAR COLLIDER USING CONVENTIONAL TECHNOLOGY*

GREGORY A. LOEW

Stanford Linear Accelerator Center
Stanford University, Stanford, California, 94305

Invited talk presented at the SLAC Summer Institute on Particle Physics
Stanford, California, July 29 – August 9, 1985

* Work supported by the Department of Energy, contract DE – AC03 – 76SF00515.

1. Introduction

In the series of reviews devoted to the future of $e^{\pm}$ linear colliders in these proceedings,[1] this article focuses on the design of a machine with a center-of-mass energy of 1 TeV which uses conventional technology. By conventional technology here is meant that the process of acceleration is achieved as is usual in common electron linear accelerators, namely that the electron and positron bunches receive their energy from RF fields stored in copper structures at room temperatures. The RF power is generated by a separate self-contained device such as a klystron or other microwave tube. This process contrasts with more futuristic schemes described in the other articles which use wakefields, plasmas and/or lasers. The 1 TeV c.m. energy (ten times that of the SLC) was chosen because it falls into an intermediate range where, as will be seen, the conventional techniques can conceivably still be used although they must be "stretched" to their capacity, but above which different regimes are entered and new approaches are clearly required.

The main building blocks of a "generic" $e^{\pm}$ linear collider are shown in Fig. 1(b), side-by-side with the SLC [Fig. 1(a)]. As is seen, the two machines contain all the same basic elements. The only fundamental difference is that in the SLC, one linac is used for both beams, and their energy is sufficiently low that it is possible within the available real estate to bend them around separate arcs to their final interaction point. At 50 GeV, the energy lost to synchrotron radiation in these arcs is about 1.5 GeV/beam. In the "generic" collider, all the building blocks are laid out along a straight line. "Damping" systems to produce the appropriate small emittances are assumed for both beams before they are launched into the main linacs. Note that it may be possible in the future to design an electron gun and injector capable of producing a beam with a low enough emittance that the electron "damping" system would not be necessary or at least could be much simpler than the positron "damping" system. The latter, on the other hand, is likely to be quite complicated and costly.

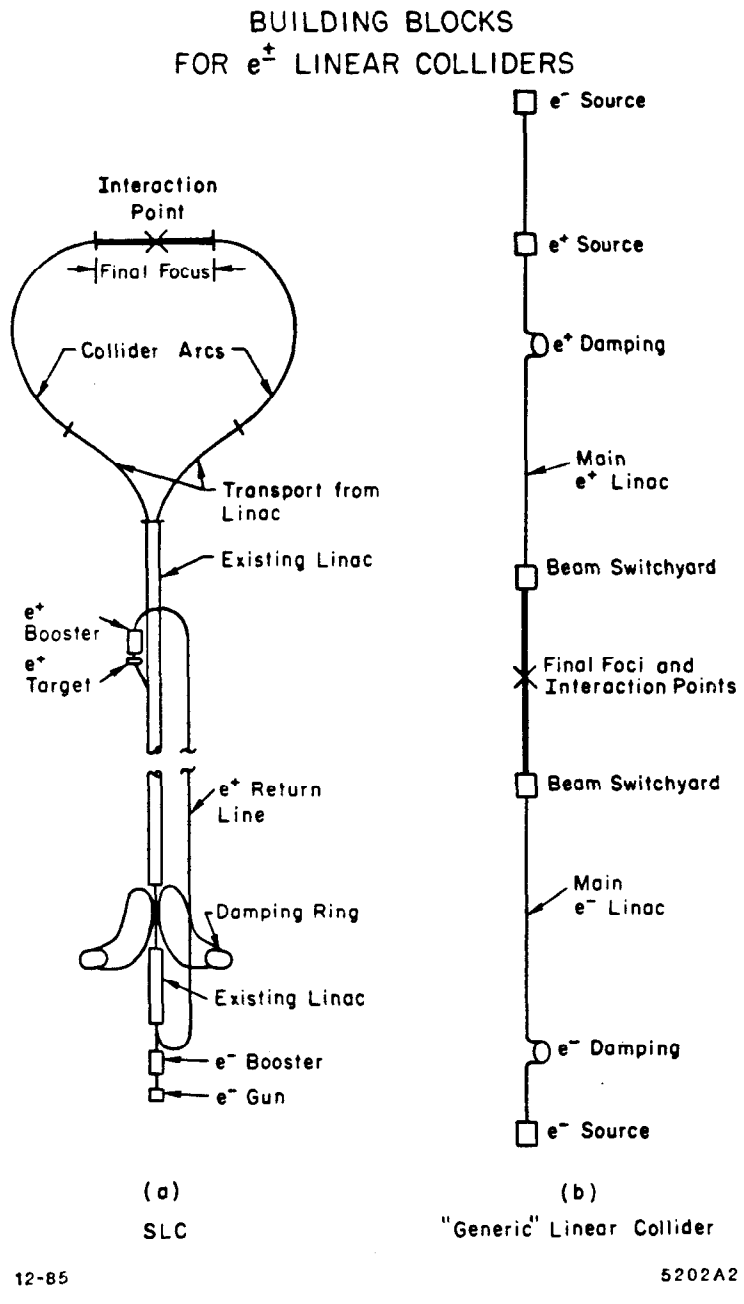

Figure 1. Building blocks for $e^{\pm}$ linear colliders: (a) SLC; (b) "Generic" linear collider.

Possible layouts of the beam switchyards, final foci and interaction points are shown in Fig. 2. Three alternates are presented. It may seem premature to consider these details at such an early stage except for the fact that the layout of the interaction points and the method of acceleration and beam dynamics in the machines strongly affect each other. Figure 2(a) illustrates a scheme where two trains of bunches of equal energies meet head-on at one interaction point. In this scheme it is possible to switch the beams from one interaction point to another, thereby doing experiments in separate detectors on a time-multiplexed basis. This system, however, can work only if all the bunches in each train have the same energy. As will be seen later, this is only possible if the linac structure is replenished with energy at the same rate as successive bunches deplete it. Alternatively, in Fig. 2(b) it is assumed that the bunches in the trains have an energy difference such that the banks of DC magnets in the beam switchyards can deflect them exactly into separate parallel channels, final foci and interaction points. Finally, Fig. 2(c) shows a serial array of interaction points where, depending on the firing time of the respective injectors, the bunches in each train can meet at a uniquely, pre-determined point. This scheme has the advantage of not requiring any major bending of the beams (except perhaps if there are chromatic correctors in the final foci) and thus being fairly energy independent. On the other hand, it is less flexible because it does not allow quick switching of the beams between interaction points, or doing set-up work in one of them while the beams are interacting in another.

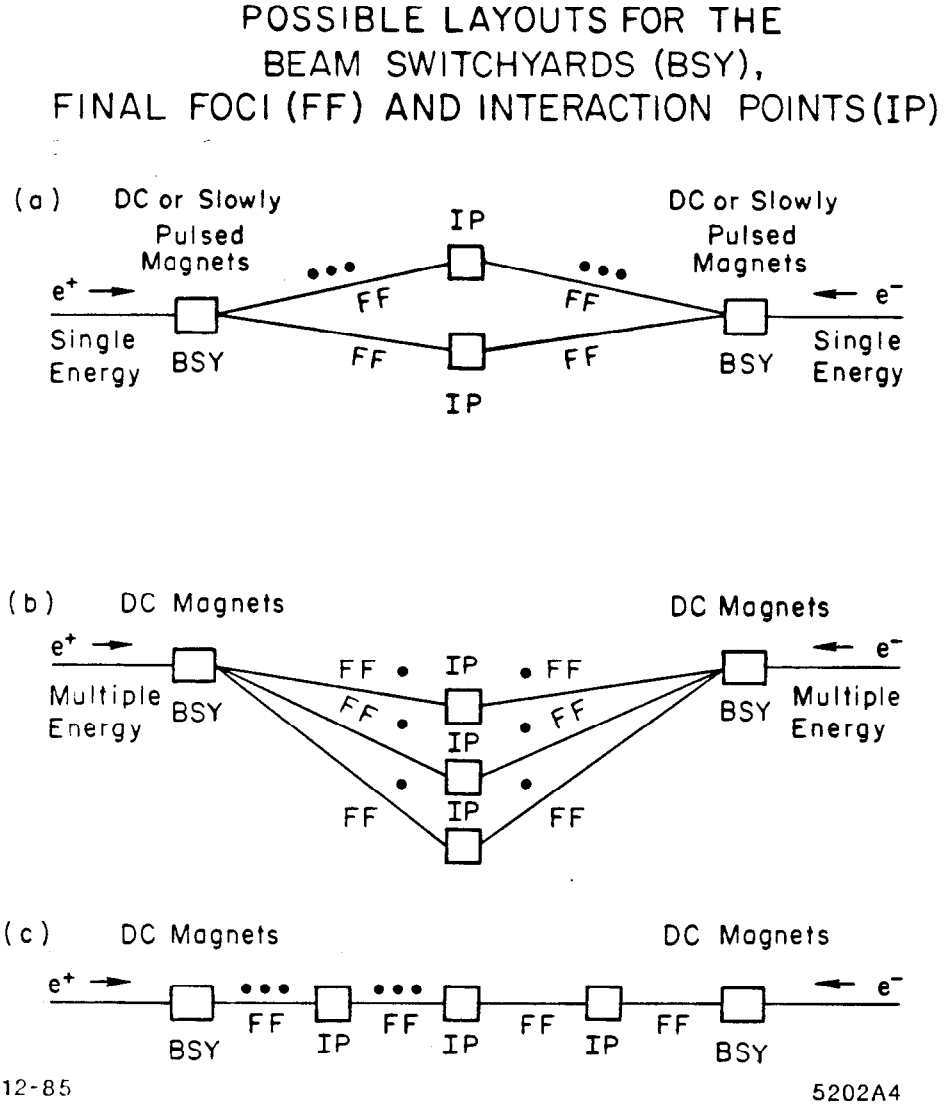

Figure 2. Possible layouts for the beam switchyards, final foci and interaction points in a high energy $e^{\pm}$ linear collider: (a) train of bunches of equal energies directed to one of several parallel interaction points; (b) train of bunches of different energies directed to several parallel interaction points; (c) train of bunches of similar energies directed to one of several interaction points in series.

2. Beam Related Parameters

The design of an $e^{\pm}$ linear collider of a given energy and luminosity is a highly iterative process in which a very large number of interdependent parameters must be selected.[2,3] The process involves a balancing act between what seems physically possible, technically reasonable and fiscally affordable. Even though the major parameters from the injectors to the final interaction point(s) are interdependent, we will try here to arrive at an overall design by dividing these parameters into those related specifically to the beams and those related to the linacs. The former are considered in this section, the latter will be discussed in the next.

As shown in Ref. 2, it is possible to affect certain key beam parameters such as the disruption parameter D and the beamstrahlung parameter δ by choosing tri-gaussian bunches in which the transverse dimensions σ_x and σ_y are not equal, i.e., the beam cross-sections are not round. Certain advantages can be achieved as one departs from round beams. However, this choice also leads to considerable complications, both computational and practical. For this reason, in the discussion below, only round beams ($\sigma_x = \sigma_y \equiv \sigma_r$) will be considered. Note that the choice of the third dimension, σ_z, is probably one of the most crucial ones because it links the beam parameters with the linac parameters: indeed, σ_z is on the one hand involved in the expressions for D and δ, and on the other hand places a lower limit on the RF wavelength that can be used.

The key beam parameters are given by the following expressions:

Luminosity

$$\mathcal{L} = fb\frac{N^2}{4\pi\sigma_r^2}H(D) = fb\frac{N^2\gamma}{4\pi\epsilon_n\beta^*}H(D) \quad , \tag{1}$$

Disruption parameter

$$D = \frac{\sigma_z}{\mathcal{F}} = \frac{r_e\sigma_z N}{\gamma\sigma_r^2} = \frac{r_e\sigma_z N}{\epsilon_n\beta^*} \quad , \tag{2}$$

Classical beamstrahlung parameter

$$\delta_{CL} = \frac{0.22\, r_e^3\, N^2 \gamma^2}{\sigma_z \epsilon_n \beta^*} H(D) \quad , \tag{3}$$

Beam power for both beams

$$2P_B = 2fb\, N\gamma\, m_0 c^2 \quad . \tag{4}$$

In these expressions,[2] the transverse dimension of the beam, σ_r, is related to the invariant emittance ϵ_n and the beam envelope parameter β^* at the interaction point by the relation

$$\sigma_r = \left(\frac{\epsilon_n \beta^*}{\gamma}\right)^{1/2} \quad . \tag{5}$$

The factor $H(D)$ is the luminosity enhancement function due to the pinch effect. N is the number of particles per bunch, r_e is the classical radius of the electron (8.85×10^{-15} m), f is the repetition frequency, b is the number of bunches per RF pulse, and $\mathcal{F}$ is the focal length of the lens produced by a bunch for a particle near the axis in the opposing bunch.

The first column of Table 1 gives the approximate beam parameters for the SLC. $\mathcal{L}_{DES}$ is the desired luminosity that is dictated by the needs of experimental physics. At the bottom of the column is shown $\mathcal{L}_{ACT}$, the luminosity that results from substituting the relevant parameters into Eq. (1). The luminosity desired for a 1 TeV c.m. $e^{\pm}$ collider must be at least two orders of magnitude higher, i.e. $\sim 2 \times 10^{32}$ cm^{-2}s^{-1} because the cross-sections of the physical phenomena of interest fall off as the square of the energy. We see then that if we do not make any excursions away from the SLC except to increase the number b of bunches by a factor of 10 (see first 1 TeV column), the beam power increases by 100. Since the linac RF and AC power must inevitably grow accordingly, this is an undesirable choice. The parameters shown in the second column are based on reductions

of the invariant emittance by a factor of 3, of the number of particles N by a factor of 2 and of the repetition rate f by 2/3. The enhancement factor $H(D)$ is increased by a factor of 2. None of these changes are drastic, yet they reduce the beam power by a factor of 3. The beamstrahlung parameter, $\delta = 0.13$, is still acceptable and remains in the classical regime. Note that the beam radius at the interaction point, σ_r, has been decreased by a factor of 5 because of the higher energy and the reduced emittance, but not because of any assumed reduction of β^*.

Table 1. Beam Related Parameters Round Beams

	SLC	1 TeV (c.m.)	
$E_{c.m.}$ (GeV)	2×50	2×500	
$\mathcal{L}_{DES}$ (cm^{-2} sec^{-1})	$\sim 2 \times 10^{30}$	$\sim 2 \times 10^{32}$	
		↙	↘
$N(e^{\pm})$/bunch	5×10^{10}	5×10^{10}	2.5×10^{10}
f (pps)	180	180	120
b (bunches/pulse)	1	10	10
β^* (cm)	0.75	0.75	0.75
$\epsilon_n = \gamma\epsilon$ $(m_0c - m)$	3×10^{-5}	3×10^{-5}	1×10^{-5}
$\sigma_r = \left(\frac{\epsilon_n\beta}{\gamma}\right)^{1/2}$ (μm)	1.5	0.47	0.27
σ_z (mm)	1	1	1
$D = \frac{r_e\sigma_z N}{\epsilon_n\beta^*}$	0.64	0.64	1
$H(D)$	~ 1.5	~ 1.5	~ 3
$\mathcal{L}_{ACT}$	2.4×10^{30}	2.4×10^{32}	2.4×10^{32}
$2P_B = 2fbNE$	144 kW	14.4 MW	4.8 MW
δ_{CL}	0.8×10^{-3}	0.8×10^{-1}	0.13

It could be argued that one would obtain a more "daring" design if instead of reducing the invariant emittance by a factor of 3, one were to decrease it by a whole order of magnitude, or even more.[3] This, however, will not be attempted here.

3. Linac Related Parameters

We will now discuss the main issues involved in the design of the linacs. These include the gradient and resulting energy stored, the type of accelerating structure, structure efficiency, peak power, pulse length, frequency dependence, types of RF sources, energy compression, system efficiency, wakefields, energy spread, focusing, alignment tolerances, Landau damping, bunch trains and overall design options.

3.1 Accelerating Gradient and Energy Stored

Let us begin, perhaps somewhat arbitrarily, with the choice of the accelerating gradient G. This choice is crucial because, for a given desired $e^{\pm}$ energy, the gradient determines the length L of the machine. From the usual definitions of shunt impedance per unit length r and Q of the accelerating structure[4] we know that

$$\omega \frac{r}{Q} = \frac{G^2}{W} \tag{6}$$

where ω is the radial frequency and W is the energy stored per unit length. The quantity $\omega r/4Q$ which scales as ω^2 is often called k_1, where the subscript denotes the fundamental space harmonic of the periodic structure which propagates at the velocity of light in synchronism with the particles.[2]

From these expressions we see that the total energy stored per linac before the beam is injected is given by

$$\bar{W}L = \frac{\bar{G}^2 L}{4k_1} = \frac{E\bar{G}}{4k_1} \tag{7}$$

where $\bar{W}$ and $\bar{G}$ are average values of the stored energy per unit length and gradient, respectively. Equation (7) shows that for a given particle energy E, the total stored energy scales as $\bar{G}$. Getting this energy to be stored in the structure requires a given filling time during which RF losses inevitably take place in the copper walls. These losses as well as the losses incurred in generating the RF from AC power must be added to the total energy budget. Thus there is a double incentive to minimize $\bar{W}L$ and maximize all the conversion efficiencies.[4,5]

There is, however, a lower limit to the energy that must be stored in the accelerator, which is determined by the energy that the beam can remove from it. If these two quantities were equal, the last electron accelerated in a bunch or bunch train would acquire zero energy. We will see later that in order to get a bunch train of reasonably uniform energy, the energy removed by the beam should be on the order of 10% of the stored energy.

Reference 2 contains a discussion on the physical limitations of accelerating gradients. The main points are summarized in Fig. 3. An experiment with a short standing-wave structure has been done at SLAC[6] at $\lambda = 10.5$ cm (2856 MHz) which gave a limit of about 150 MV/m accelerating field and over 300 MV/m peak surface field on the copper disks. At this level, there was a large amount of field emitted current inside the structure, and x-ray radiation surrounding it (close to a Megarad/hr average on the side of the accelerator at 120 pps and 2.5 μsec RF pulse length). Work is presently being planned at other frequencies (C- and X-band) to determine if the predicted $\omega^{7/8}$ dependence shown in Fig. 3 is correct. In any case, it is certainly desirable to stay below these limits for reliable operation of an accelerator. The consequences of choosing a particular gradient will become apparent later by illustration of several examples.

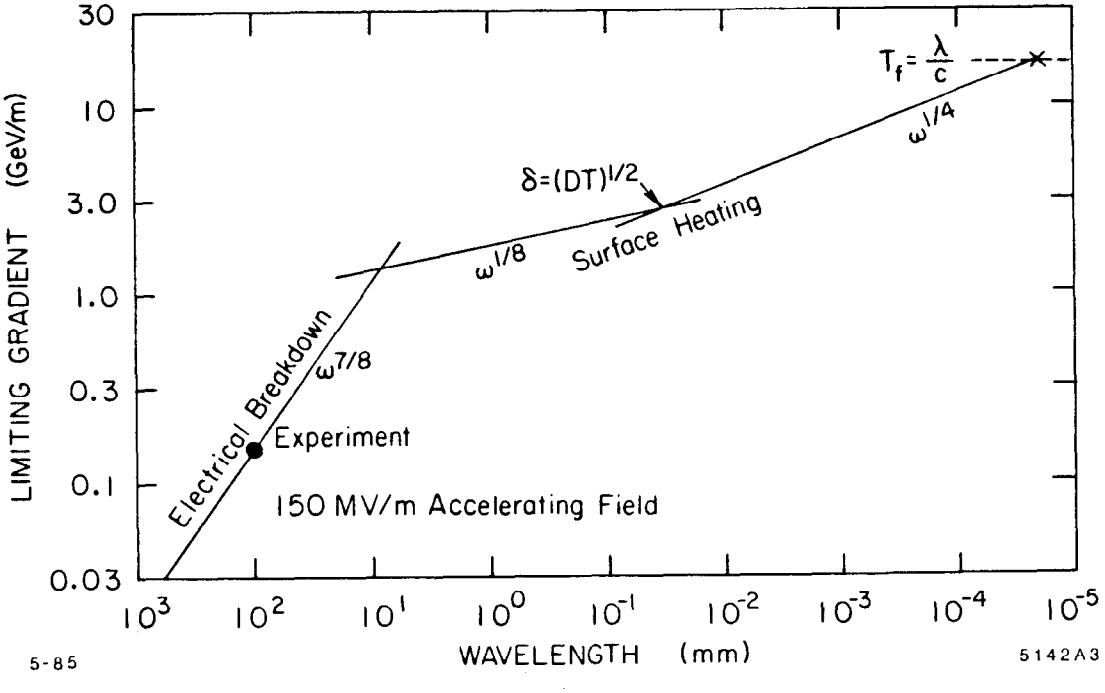

Figure 3. Limiting accelerating gradient as a function of RF wavelength.

3.2 Traveling-Wave Versus Standing-Wave Structures

There are basically two types of accelerator structures: traveling-wave (TW) and standing-wave (SW).[4] The choice between them is not clear. The TW structure has the advantage that it delivers a constant no-load accelerating voltage after one filling time and that it does not produce any reflections back towards the klystron, but it requires an extra output load to absorb the left-over power. In contrast, the SW structure does not require any output load but it does present reflections to the klystron while it is filling. The reflections can be made to cancel if the klystron feeds two sections in parallel whose inputs are 90 electrical degrees apart, but then a 3 db hybrid with a load in the fourth arm is needed as a power splitter. The SW structure approaches its final accelerating voltage asymptotically if a constant input power is applied. For practical purposes it reaches 99% of its final voltage in about five filling times.

Most of the other similarities and differences can best be understood by taking a section of length ℓ and by comparing the expressions giving the attainable voltage V, the energy Pt supplied to the input of the section by a peak power P during a pulse of length t, the energy W_ℓ stored in the section, and the structure efficiency, η_{ST}, defined here as the ratio of energy stored to energy supplied. In the case of the TW structure, sections can be of the uniform (or constant impedance) type in which the field decays exponentially with length, or of the constant gradient (linearly decreasing group velocity) type in which the field remains constant as a function of length.[4] The key expressions are given below.

TW, Constant Impedance:

$$V = \frac{1 - e^{-\tau}}{\tau} (2\tau)^{1/2} (Pr\ell)^{1/2} \tag{8}$$

$$Pt_F = \left(\frac{\tau}{1 - e^{-\tau}}\right)^2 \frac{V^2}{\omega \frac{r}{Q} \ell} \tag{9a}$$

$$\rightarrow (1+\tau)\,\frac{V^2}{\omega\frac{r}{Q}\ell} \qquad \text{when } \tau \text{ small} \tag{9b}$$

$$W_\ell = \frac{\tau\left(1-e^{-2\tau}\right)}{2\left(1-e^{-\tau}\right)^2}\,\frac{V^2}{\omega\frac{r}{Q}\ell} \tag{10}$$

$$\eta_{ST} = \frac{1-e^{-2\tau}}{2\tau} \tag{11a}$$

$$\rightarrow (1-\tau) \qquad \text{when } \tau \text{ small} \tag{11b}$$

TW, Constant Gradient:

$$V = \left(1-e^{-2\tau}\right)^{1/2}\,(Pr\ell)^{1/2} \tag{12}$$

$$Pt_F = \left(\frac{2\tau}{1-e^{-2\tau}}\right)\,\frac{V^2}{\omega\frac{r}{Q}\ell} \tag{13a}$$

$$\rightarrow (1+\tau)\,\frac{V^2}{\omega\frac{r}{Q}\ell} \qquad \text{when } \tau \text{ small} \tag{13b}$$

$$W_\ell = \frac{V^2}{\omega\frac{r}{Q}\ell} \tag{14}$$

$$\eta_{ST} = \frac{1-e^{-2\tau}}{2\tau} \tag{15a}$$

$$\rightarrow (1-\tau) \qquad \text{when } \tau \text{ small} \tag{15b}$$

In these expressions τ is the attenuation of the section $(\omega\ell/2v_gQ)$ and t_F is the filling time $(2Q\tau/\omega)$ after which steady state is reached and the beam can be injected. We will see later that when a bunch train is used, one can inject the first bunch before the section is entirely filled,[5] in such a way that the incremental energy stored during bunches n and $n+1$ is equal to the energy removed by bunch n. If this compensation can be made exact, all bunches in the train then

acquire the same energy, as assumed in Fig. 2(a). A similar idea can be used for SW structures. Both are illustrated later in Fig. 12.

Note that the expressions for η_{ST} in Eqs. (11) and (15) are identical. The definition for the structure efficiency chosen in Refs. 2 and 7 $[V^2(0)/V^2(\tau)]$ gives a slightly different expression for the constant impedance case $[((1-e^{-\tau})/\tau)^2]$ but the same as (15) for the constant gradient case. The numerical results in the range of interest for τ are the same within a few percent.

Traveling-wave structures are generally built with cavities of length $\lambda/4$ or $\lambda/3$ ($\pi/2$ or $2\pi/3$ phase shift per period) around which the shunt impedance has a broad maximum. To give an idea of the orders of magnitude involved, in the middle of the SLAC constant-gradient disk-loaded structure the quantities of interest have the following values:

Frequency	F	=	2856 MHz
Phase shift per period	ϕ	=	$2\pi/3$
Cavity diameter	$2b$	=	8.27 cm
Iris diameter	$2a$	=	2.34 cm
Disk thickness	t	=	0.58 cm
Normalized group velocity	v_g/c	=	0.0134
Shunt impedance	r	=	57 MΩ/m
	Q_0	=	13,700
	r/Q	=	4160 Ω/m
	k_1	=	18.6×10^{12} V/C-m

The integrated value of τ for a length $\ell = 3.05$ m of 86 cavities is 0.57 and the filling time is 0.83 μsec. At a given frequency, v_g/c varies roughly as $(a/b)^4$, r as $\sim (a/b)^{-1/2}$ and k_1 as $\sim (a/b)^{-1}$.

Standing-wave structures are generally built with a zero group velocity and π-phase shift per cavity, or preferably with a high group velocity (5 to 15% of c) and a $\pi/2$-phase shift per cavity, except that every second cavity has no interaction or

very little interaction with the beam (by being either off-axis or very short, and unexcited). The high group velocity means that the power travels very rapidly and with very little loss through the structure so that the fields build up equally and almost simultaneously in all the excited cavities. The build-up takes place through rapid multiple reflections back and forth, and one defines a filling time t_F as:

$$t_F = \frac{2Q_L}{\omega} = \frac{2Q_0}{(1+\beta)\omega} \tag{16}$$

where Q_0 is the unloaded Q of the structure, Q_L is the loaded Q $[Q_0/(1+\beta)]$ and β is the coupling coefficient of the structure to the input waveguide, defined as

$$\beta = \frac{\text{Power emitted through the coupling hole}}{\text{Power lost to the walls of the structure}} \tag{17}$$

The attainable voltage for the SW structure then is:

$$V = \left(1 - e^{-(t/t_F)}\right) \frac{2\beta^{1/2}}{1+\beta} (Pr\ell)^{1/2} \tag{18}$$

The energy Pt needed to reach the voltage V can be shown to be minimized[7] when $t = 1.257\, t_F$ in which case

$$Pt = 1.228(1 + \frac{1}{\beta}) \frac{V^2}{\omega \frac{r}{Q} \ell} \tag{19}$$

Then

$$W_\ell = \frac{V^2}{\omega \frac{r}{Q} \ell} \tag{20}$$

and

$$\eta_{ST} = \frac{1}{1.228} \left(\frac{1}{1 + \frac{1}{\beta}} \right) \tag{21a}$$

$$\rightarrow \frac{1}{1.228} \left(1 - \frac{1}{\beta}\right) \qquad \text{when } \beta \text{ large} \tag{21b}$$

Comparing expressions (9b), (13b) and (19) as well as (11b), (15b) and (21b), we see that there is a one-to-one correspondence between τ (when τ small) and $\frac{1}{\beta}$ (when β large): in the TW cases, the attenuation is low, the group velocity is high and the power propagates rapidly through the section with little loss; in the SW case, the section is "over-coupled" and the fields build up rapidly to their final value although this value is not as high as it would be if β were equal to 1 ("critical coupling"). Because of the mis-match, 22.8% of the energy is reflected at the input and never gets into the section. One might conclude from this that the TW structures are inherently better than the SW ones. However, it turns out that the values of r and r/Q can be made 25 to 40% higher ($r \sim 80$ MΩ/m and $r/Q \sim 5500$ Ω/m) for the SW structures by using irises with a smaller diameter (2a) and nose cones which improve the transit time factor through the cavities. As a result, it is not clear at this time whether TW or SW structures are better suited for future linear colliders. The choice may be influenced more by other issues such as ease and cost of fabrication.

3.3 Structure Efficiency, Peak Power, Pulse Length and Frequency Dependence

Figure 4 shows the structure efficiency and normalized peak power per unit length as a function of τ for the constant gradient case. The structure efficiency, η_{ST}, is given by Eq. (15a) and the normalized power, $(P/\ell)/(G^2/r)$ which is equal to $(1 - e^{-2\tau})^{-1}$, is obtained from Eq. (12). It is seen that there is a trade-off between the two quantities: for large τ, the required peak power per unit length to obtain a given gradient is comparatively small but the structure efficiency is poor, and *vice-versa* for small τ. A small value of τ [$\tau = (\omega\ell)/(2v_gQ)$] arising from a larger group velocity implies that the pulse from the RF source can be short but its peak power must be large for a given desired energy stored and voltage gain. The value of $\tau = 0.57$ chosen for the SLAC structure is actually a reasonable compromise: it gives a structure efficiency of about 59% and a normalized peak power per unit length of 1.47.

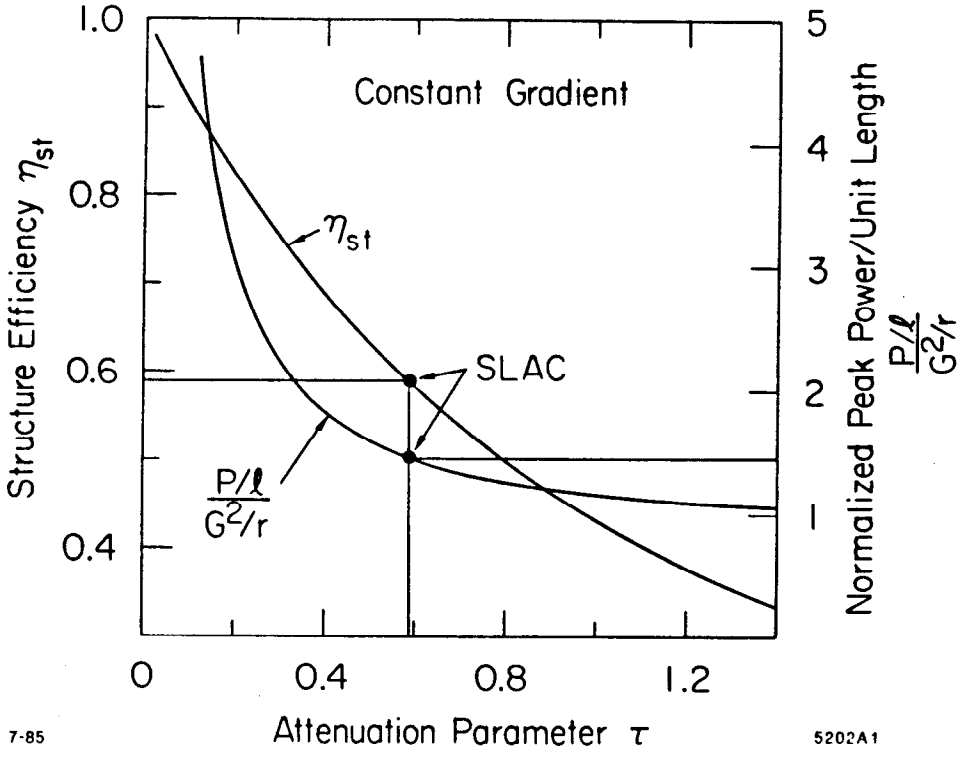

Figure 4. Structure efficiency and normalized peak power as a function of attenuation parameter τ for constant gradient structures (note SLAC case for $\tau = 0.57$).

Let us now examine the frequency dependence of these quantities. If we assume constant τ, v_g and G, the following scaling rules apply:

$$\begin{aligned} r &\sim \omega^{1/2} \\ Q &\sim \omega^{-1/2} \\ \frac{r}{Q} &\sim \omega \\ k_1 &\sim \omega^2 \\ W &\sim \omega^{-2} \\ t_F &\sim \omega^{-3/2} \\ \ell &\sim \omega^{-3/2} \\ P/\text{section} &\sim \omega^{-2} \\ P/\text{meter} &\sim \omega^{-1/2} \end{aligned} \tag{22}$$

Note that whereas the peak power per section of length ℓ and attenuation τ decreases as ω^{-2}, the peak power per unit length decreases only as $\omega^{-1/2}$.

From all the above expressions, we can obtain the peak power and filling time as a function of frequency or wavelength. This has been done[7] for a typical disk-loaded structure ($\tau = 0.5$) at several values of the gradient G, and the results are shown in Fig. 5. The points indicated as 0 through 5 represent the cases which will be used later as examples in Table 2. Perhaps the most crucial observation to be made from this figure is that for linacs of reasonable total length and thus of relatively high gradient, the peak powers required per meter will be in the several hundreds of megawatts unless one can go to frequencies at least an order of magnitude higher than SLAC. Filling times would then come down by a factor of 30: this is good from the point of view of energy conservation but would require new approaches to the problem of generating the increasingly high voltages necessary to pulse the RF sources and avoiding inefficiencies during the inevitable rise and fall times of the pulses. Also, the trend towards higher frequencies would lead to much shorter and more numerous accelerator sections and thus to a much greater number of feeds, power splitters, couplers and loads.

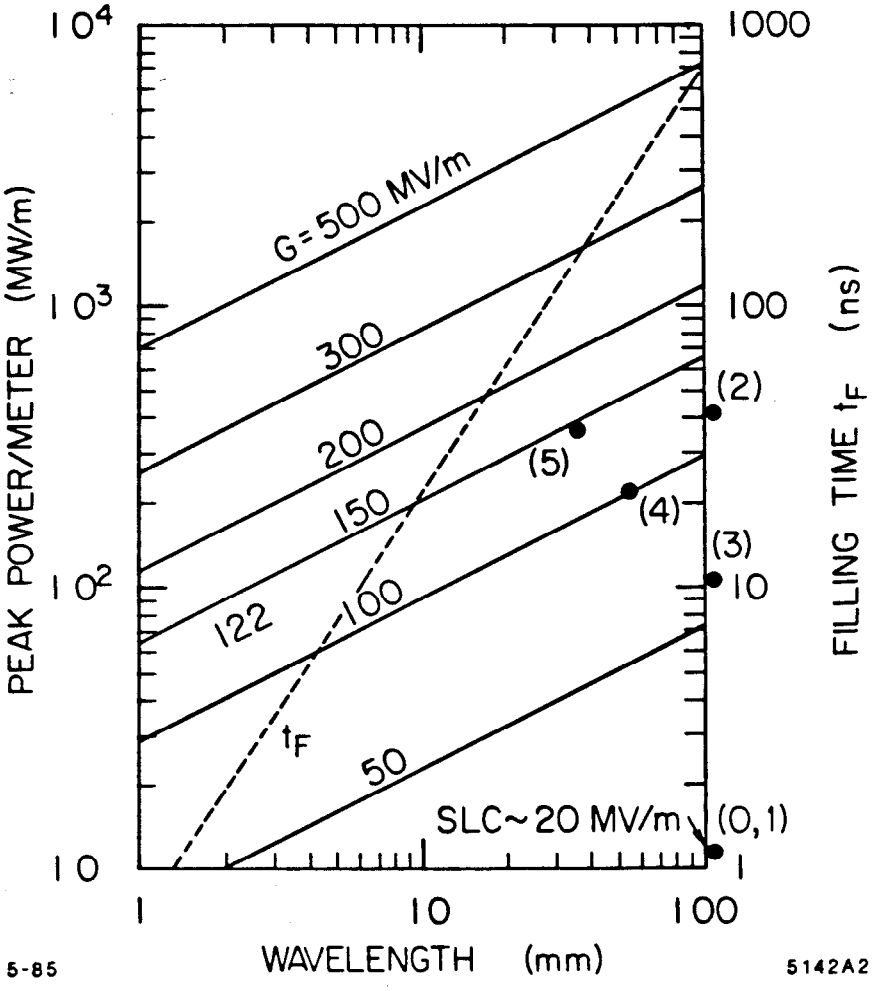

Figure 5. Peak power per meter and filling time as a function of wavelength for various values of accelerating gradient for a typical disk-loaded structure ($\tau = 0.5$). The numbered points indicated in the figure refer roughly to the peak powers per meter for the examples in Table 2 ($\tau = 0.57$). The difference between the two values of τ is neglected here.

3.4 High Power Sources, Pulse Compression and Overall System Efficiencies

How is high power at microwave frequencies generated and what sources are available? At the present time, all high microwave power is produced in vacuum tubes by an electron beam of high kinetic energy formed and bunched in such a way that it interacts with and amplifies electromagnetic fields at the cost of its own original energy. The tubes differ fundamentally only in the method of beam bunching and cavity interaction, either longitudinal (klystrons) or transverse (gyroklystrons and free electron lasers).

Up to the present, all high-energy linacs have used high power klystrons, some at L-band (around 1200 MHz), most of them at S-band (around 3000 MHz). The klystrons with the highest peak power output at S-band are built and used at SLAC[8] (Model XK-5 with 36 MW peak and 36 kW average, and the more recent "SLC" klystron with up to 65 MW peak and 45 kW average, with efficiencies between 40 and 50%). Higher peak power sources with adequate average power and pulse length are only now appearing on the scene, mostly on an experimental or early developmental basis. Four examples are shown in Fig. 6. The first is a 150 MW klystron (1 μsec, 2856 MHz) of which two prototypes were recently built at SLAC within the framework of a US/Japan Collaboration.[9] The second is a so-called laser klystron or "lasertron," also under design and construction at SLAC.[10] The first model, if successful, should produce about 30 MW of peak power for 1 μsec pulses at 2856 MHz. The appeal of the lasertron is its predicted high efficiency: indeed, whereas in a regular klystron the longitudinally bunched electron beam which produces the RF energy is formed by velocity modulation and progressive interaction with several RF cavities, in the lasertron the bunching is produced at the cathode by the impinging RF modulated laser. Efficiencies in excess of 70% are expected in the process. Another advantage of the lasertron is that the pulsed modulator to produce the beam for a regular klystron can hopefully be replaced by a much simpler high voltage DC power supply. These

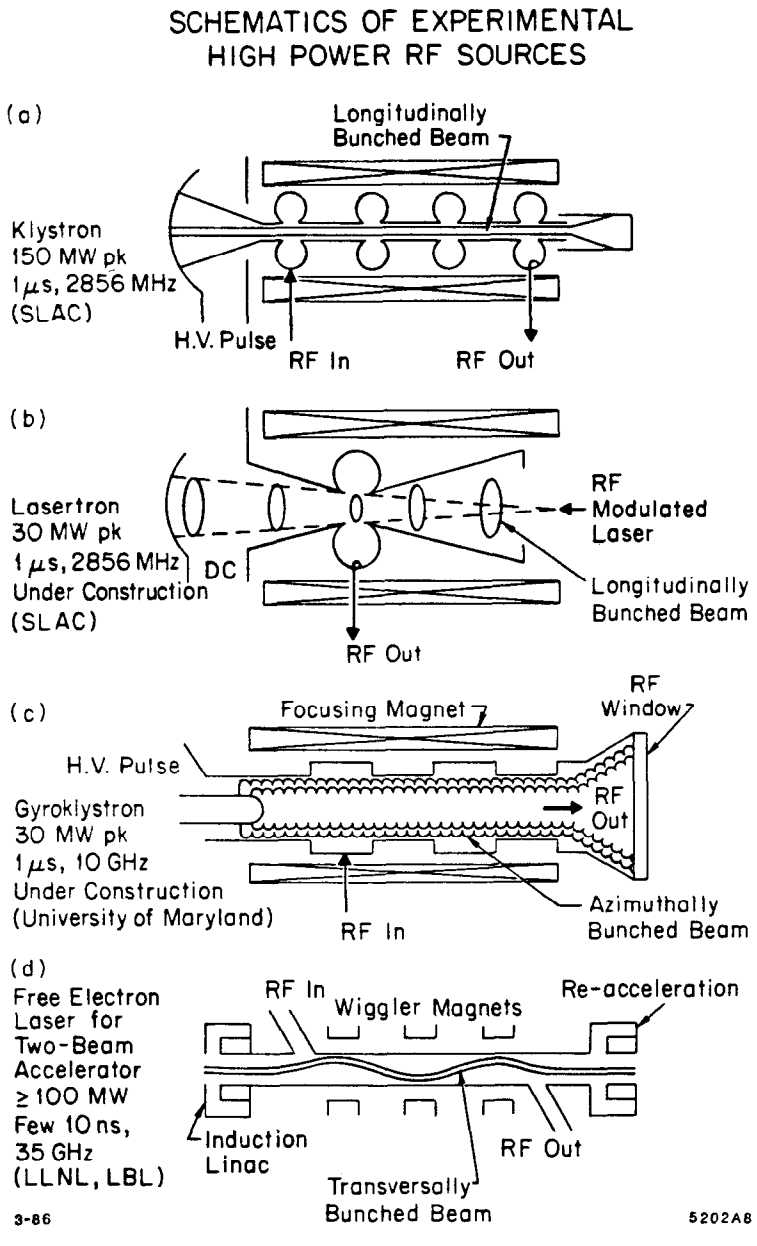

Figure 6. Schematics of experimental high power RF sources that have been proposed for high energy $e^{\pm}$ linear colliders.

advantages must, however, be weighed against the complexity of the RF modulated laser system, the photocathode and vacuum technology, and the general untested new features of the device.

As one goes to higher frequencies, the peak power available from klystrons is generally believed to drop as $\omega^{-2.5}$ because of size, beam current and breakdown of the longitudinally interacting electric fields in the cavities. Experience then shows that gyroklystrons in which the electron bunching and electric fields are azimuthal are capable of higher power. The third device shown in Fig. 6 is a gyroklystron under design and construction at the University of Maryland.[11] The first model is supposed to produce 30 MW of peak power for 1 μsec pulses at 10 GHz. The beam formed by the magnetron-type gun is hollow and the combination of transverse velocity component and longitudinal magnetic field produces helical electron trajectories as shown. The power output is generated by the azimuthally bunched beam delivering energy to the fields in a TE_{011} cavity (as opposed to the TM_{010} cavities in klystrons). The efficiency is predicted to be in the 30 to 40% range.

The fourth device in Fig. 6 is the generator part of the Two-Beam Accelerator,[12] i.e., the Free Electron Laser. It uses a 40 MeV electron beam from an induction accelerator which is caused to wiggle transversely by a static alternating magnetic field. The beam interacts with the transverse TE_{01} fields in an overmoded rectangular waveguide with periodic output couplers. The advantage of the device is that if the beam does not deteriorate unduly in the interaction, it can be periodically reaccelerated by another induction module, thus reducing the number of independent cathodes and injectors. The exact efficiency and peak power output obtained in the FEL at LLNL are not known but powers in excess of 100 MW for 10-15 nsec pulses at 34.6 GHz have been obtained. It remains to be seen whether the size and complexity of this device will make it practical for long linear colliders of modular construction.

Whatever microwave tube turns out to be practical for an $e^{\pm}$ linear collider in the TeV range, Fig. 5 indicates that an extra power boosting stage may be necessary between the source and the accelerator. For the SLC, this power booster consists of an energy compression scheme called SLED.[13] In this method each klystron charges two microwave storage cavities which are then discharged by means of a rapid 180° phase shift. The scheme achieves an effective power multiplication of 2.5 to 3.2, depending on pulse length. The resulting output power averaged over one filling time (0.83 μsec) is 156 MW, and the efficiency of the compression scheme is roughly 50%.

A different method of "piling up" energy is shown in Fig. 7. This so-called binary power multiplier, which can be used in multiple cascaded stages, is due to Z. D. Farkas.[14] It is similar to SLED in that it uses a rapid 180° phase shifter at the input. However, here the outputs of two klystrons are combined twice: after the first hybrid, a low-loss high power delay line (yet to be developed) "piles up" the energy in the upper leg so that it can be added in the second hybrid to the prompt pulse in the lower leg. In principle, power multiplications of 2, 4 and 8 are obtainable with this technique.

So far in this and the previous section, we have considered the tube, compression and section efficiencies. To complete the entire chain from the AC line to the beam, three more efficiencies must be considered: the AC-to-high-voltage (HV) efficiency, i.e., the efficiency due to energy lost in the substation and the modulator or power supply, the efficiency of the waveguide feed between the source, compressor and the structure, and the efficiency of converting stored energy to beam energy. The latter is considered in the next section. All other efficiencies are shown in Fig. 8 for the SLC power train. We see that the global efficiency, $\eta_{AC\to ST}$, is only 0.088 or less than 10%. This number is very low and will need to be improved upon considerably if an energy-viable machine is to be constructed. A goal of reaching an $\eta_{AC\to ST}$ of 0.3 or 30% will be assumed in the examples shown later in Table 2.

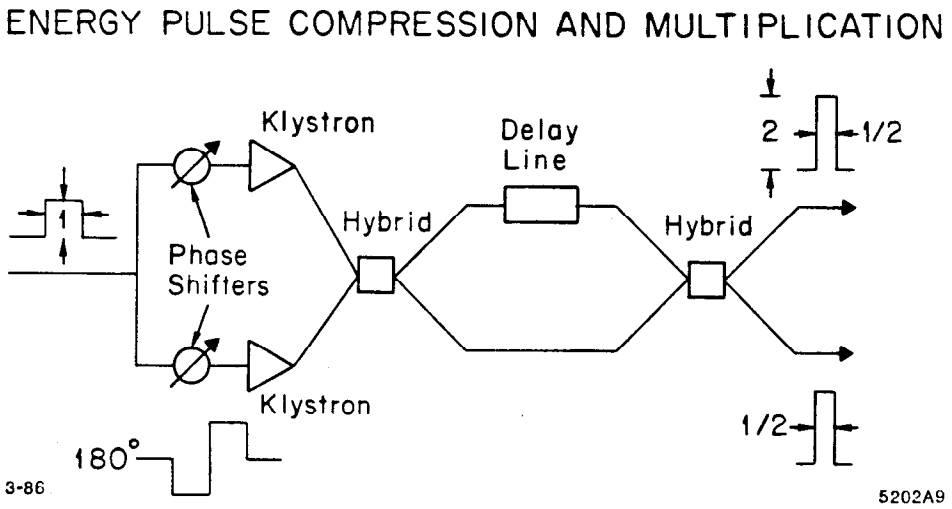

Figure 7. Single stage of an energy pulse compression and multiplication scheme which doubles the power of two sources at the expense of halving their pulse length. Several stages can be added in cascade to obtain 2^n multiplication.

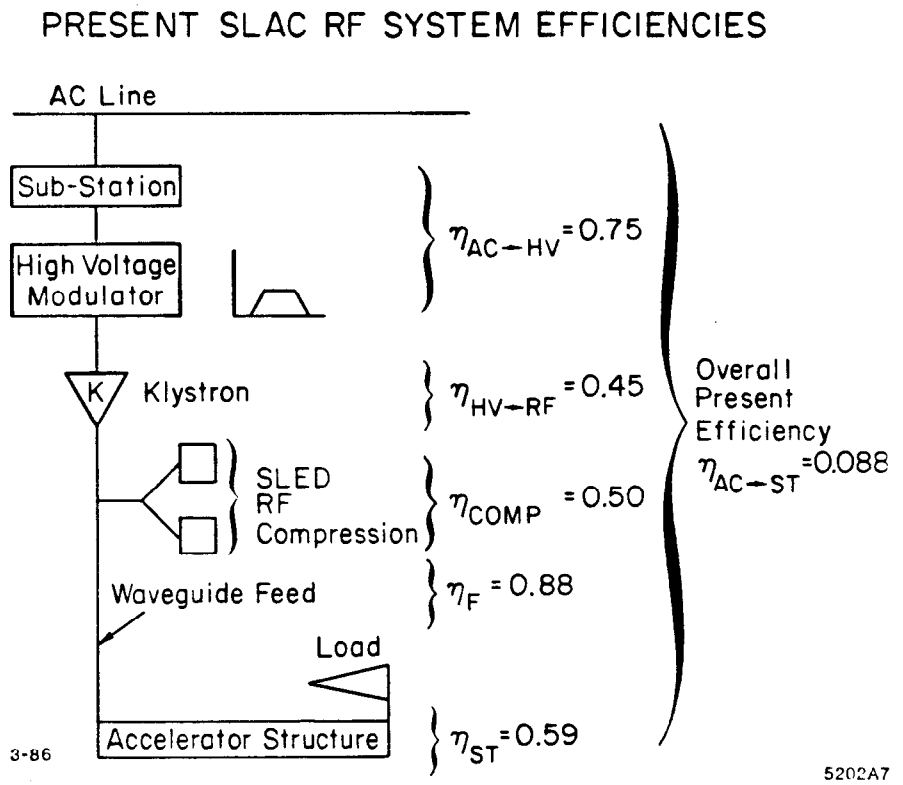

Figure 8. Present efficiencies of individual sub-systems and of global RF system used for the SLC.

3.5 Wakefields, Energy Spread Within a Bunch, Focusing, Alignment Tolerances and Landau Damping

The subject of wakefields[7,15–17] in linac structures is too lengthy to be treated here in detail and only some of the essential problems will be discussed. When $e^{\pm}$ bunches pass through a periodic structure, they leave behind them energy in the form of wakefields. These wakefields come in two forms, longitudinal fields induced with no dependence on radial bunch position, and transverse dipole fields dependent on radial bunch position. These fields are measured in terms of wake potentials which give the voltage and transverse kick versus time produced by a unit charge delta-function traversing one periodic length of structure. Figure 9 shows the cosine-like longitudinal wake and Fig. 10 the sine-like dipole wake, both computed for the SLAC constant gradient structure.[2] The longitudinal wake potential scales as ω^2 and for an otherwise fixed geometry at constant frequency roughly as $a^{-1.7}$. The dipole wake potential scales roughly as ω^3 and as $a^{-2.25}$.

The effect of the longitudinal wakefields produced by early electrons in a bunch is to decrease the energy of later electrons, as if the cylindrically symmetric image charges induced in the disks "pulled" them back. Similarly, the effect of the dipole wakefields is to distort the bunches laterally, as if the asymmetric image charges induced in the disks "pulled" the bunch tails to one side or the other, thereby making them look like bananas or even worms after some distance of interaction. In the transverse case, growth occurs because of jitter at injection, misalignments and the natural betatron motion of the bunches along the quadrupole focusing lattice of the accelerator. As the bunches become more tranversely skewed, the transverse fields they leave behind increase, and so on. The net effect is a growth in transverse emittance which results in a decrease in luminosity.

Fortunately, both effects can be controlled. The energy spread introduced in the bunch by the longitudinal wakefields can be reduced to zero by properly shaping the longitudinal charge distribution of the bunch and by placing its

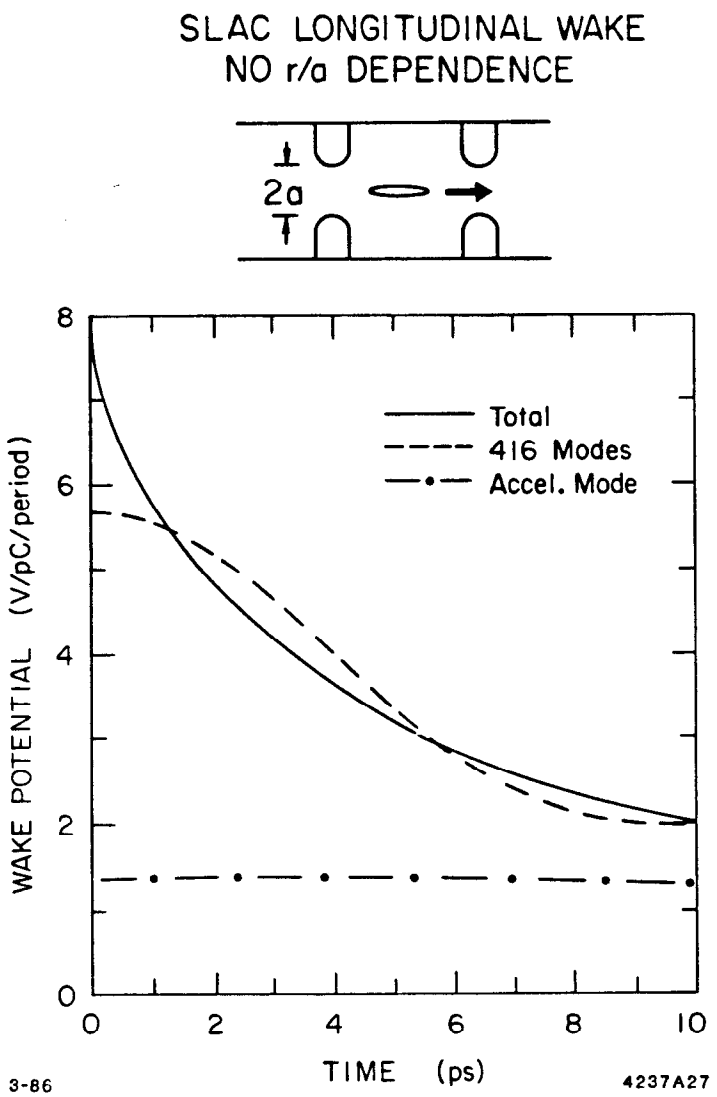

Figure 9. Wake potential as a function of time for longitudinal wakefields produced by delta-function charge traveling through "average" cavity of SLAC disk-loaded structure.

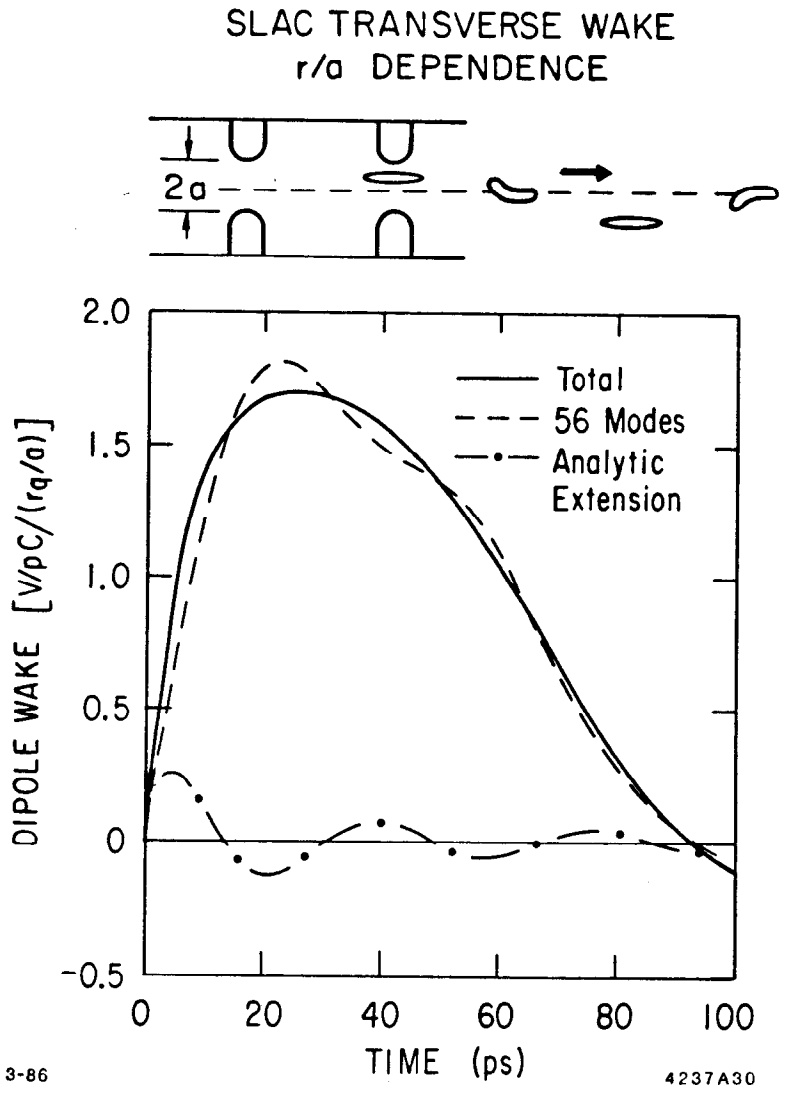

Figure 10. Wake potential as a function of time for dipole wakefields produced by delta-function charge traveling off-axis through "average" cavity of SLAC disk-loaded structure.

head at a specified angle θ_0 with respect to the crest of the accelerating wave.[18] Physically, this cancellation is possible because the net voltage induced by the wakefields is made to be exactly equal but opposite in sign to the rising slope of the sine wave at the point where the bunch is placed. Figure 11 shows examples of five bunch shapes and their respective head positions (θ_0) that have been calculated for the SLC. The letter T denotes the tail of the bunch for which the total integrated charge is $5 \times 10^{10}\, e^-$ or e^+.

The transverse emittance growth can be controlled by minimizing position and angular injection errors and jitter, by increasing the focusing strength of the lattice so that the bunches can never travel very far from the accelerator axis, by controlling misalignments of accelerator sections and quadrupoles, and by using a technique called Landau damping. In the SLC for example, alignment tolerances are on the order of 50-100 μm. The quadrupole FODO lattice immediately downstream of injection from the damping rings has an average β-function of a few meters ($\beta_{max} \sim 10$ m, $\beta_{min} \sim 2$ m). The Landau damping[19] which is being planned consists of starting off the bunches behind the accelerating crest so that the electrons in the head have substantially more energy than those in the tail. The resulting energy spread causes the electrons in the tail to have a different betatron tune or wavelength than the driving ones in the head. The effect of this shift is to substantially dampen the resonant growth that otherwise would take place as a result of initial position or angular jitter. The only apparent disadvantage of Landau damping is that after some distance of travel, it is necessary to take out the energy spread introduced in the bunch by flipping it ahead of crest where the inverse correlation takes place. The global effect is a net loss of energy gain, on the order of 1 GeV in the SLC.

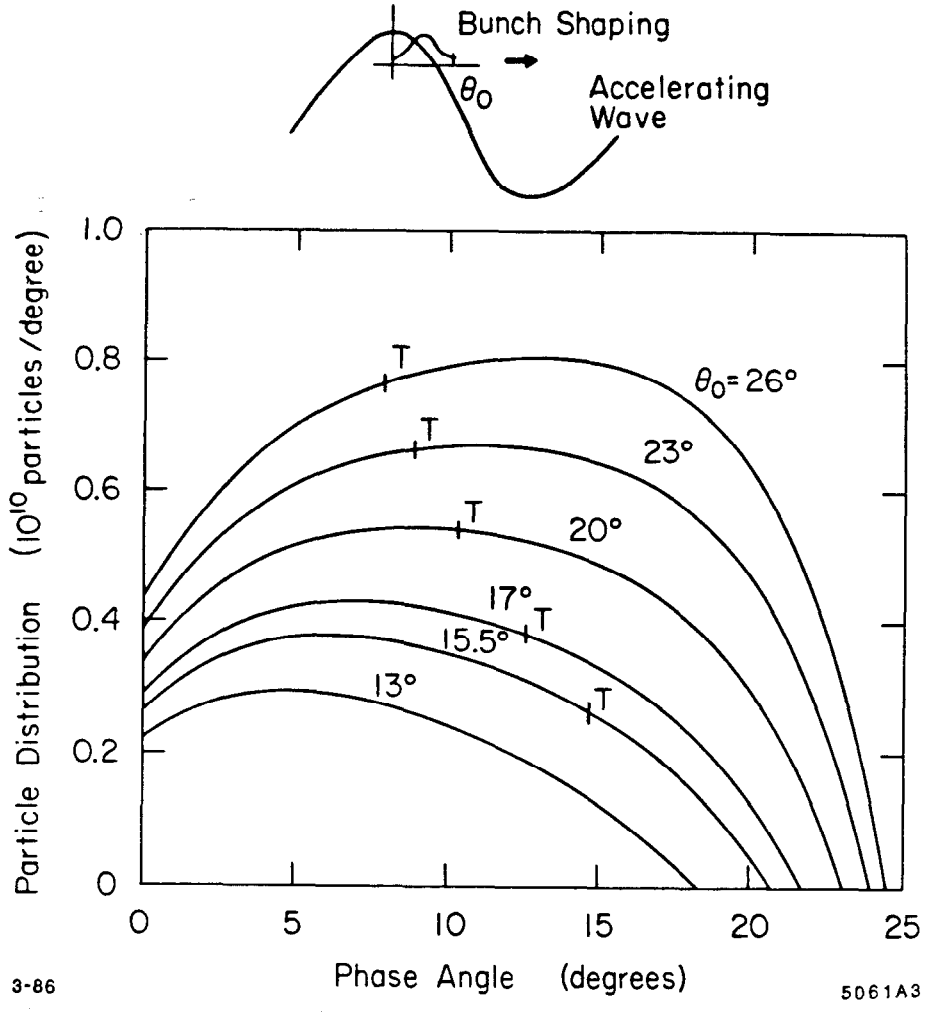

OPTIMUM BUNCH SHAPES
FOR $\Delta E/E \rightarrow 0$

Figure 11. Examples for the SLAC structure of five bunch shapes, each starting with the bunch head at a given angle θ_0, for total energy spread cancellation within the bunch. The letter "*T*" designates the point where the integrated charge in the bunch reaches $5 \times 10^{10}\, e^{\pm}$. Note that for the $\theta_0 = 13°$ case, the shape is such that the bunch cannot reach this charge.

3.6 Bunch Trains and Ultimate Beam Efficiency

The obvious reason for using bunch trains rather than single bunches is to make better use of the energy stored in the accelerator during a given pulse. If a single bunch of charge Ne rides on a wave of gradient G at an average angle θ_0, the energy it gains per unit length is

$$W_B = Ne\,G\cos\theta_0$$

and the ultimate efficiency of energy transfer from the structure to the beam is

$$\eta_{ST\to B} = \frac{Ne\,G\cos\theta_0}{W}$$

but since $W = G^2/4k_1$ [Eq. (7)],

$$\eta_{ST\to B} = \frac{4Ne\,k_1\cos\theta_0}{G}$$

For a train of b bunches of the same energy, the efficiency becomes

$$\eta_{ST\to B} = \frac{4b\,Ne\,k_1\cos\theta_0}{G} \tag{23}$$

Actually, this expression does not quite represent the complete physical situation and requires some discussion. Indeed, the exact energy acquired by the bunches depends on the so-called beam loading caused by the wakefields and the time of injection.

When a point charge q travels along the axis of an unexcited section of accelerator, it loses an energy $k_T q^2$ per unit length, where $k_T = \sum_{n=1}^{\infty} k_n$, to the longitudinal cylindrically symmetric modes. The energy lost per electron is $k_T q$. For a bunch of Gaussian distribution of length σ_z, the expression for k_T becomes

$$k_T = \sum_{n=1}^{\infty} k_n \exp\left[-\left(\frac{\omega_n \sigma_z}{c}\right)^2\right] \tag{24}$$

but now the electrons do not all lose the same energy. As seen in the previous section, the resulting energy spread can with proper bunch shaping be cancelled

by the accelerating wave, at a net cost in efficiency equal to $\cos\theta_0$. The average energy loss per electron, however, is still $k_T q$. For example, for $\sigma_z = 1$ mm and $q = 5 \times 10^{10} e$, the loss $k_T q$ for the entire SLAC linac (2900 m) is 1.38 GeV.

A few RF cycles after passage of the bunch, the higher-order modes ($n > 1$) "de-cohere" (their different frequencies make their phases scramble) and their energy gets dissipated in the structure. Only the fundamental wave of amplitude $2k_1 q$ continues to ring and, now in the presence of the accelerating wave, it subtracts from its amplitude as "beam loading," i.e., the effective gradient after passage of the bunch is $G - 2Ne\,k_1$. For a train of b bunches, the total beam loading voltage loss per unit length is simply $2bNe\,k_1$. How do we compensate for it?

The remedy,[5] as indicated earlier, is to adjust the bunch train length t_B such that if it is injected at time $t_F - t_B$ (see Fig. 12(a)), the "missing" voltage per section ΔV given by

$$\Delta V = V\left(\frac{2\tau}{e^{2\tau}-1}\right)\frac{t_B}{t_F} \tag{25}$$

is equal to $2bNe\,k_1\ell$.

For $\tau \sim 0.5$, $\Delta V/V \sim t_B/2t_F$. If for example we want approximately 10% of the energy stored in the accelerator to be removed by the beam, then the power and energy that must be stored in the section must accordingly be increased by 10% or the factor

$$\left(1+\frac{\Delta V}{V}\right)^2 \sim \left(1+\frac{t_B}{2t_F}\right)^2 \tag{26}$$

This factor must be included in the overall efficiency formula.

Note that there are two alternative operating modes if one wants the bunches to be well separated in energy (see Fig. 2(b)). One is to inject the first bunch when the section is filled ($t = t_F$) and to extend the length of the RF pulse to $t_F + t_B$. In this case, the first bunch will see the full gradient G and the last one will see the reduced gradient $G - 2bNe\,k_1$. If we want the bunches to be

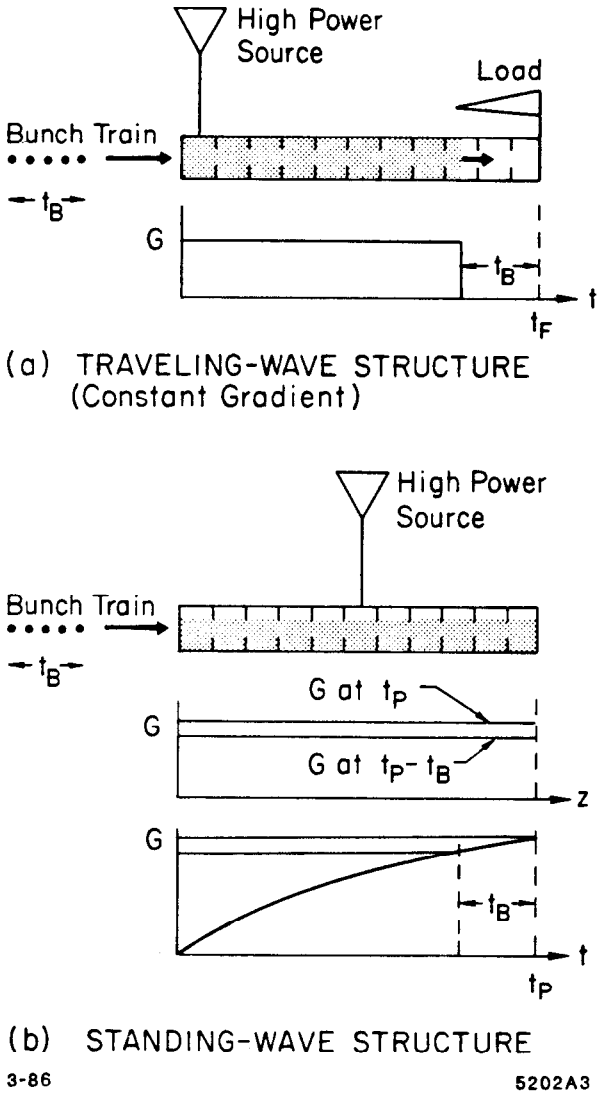

Figure 12. Multibunch injection for traveling-wave and standing-wave structures to minimize energy difference between bunches.

even more separated in energy, it is possible not to extend the RF pulse beyond $t = t_F$, in which case the tail of the RF pulse will move away from the input of the section and a further decrease in effective gradient will result as given by

$$\Delta G = G\left(\frac{2\tau}{1-e^{-2\tau}}\right)\frac{t_B}{t_F} \quad . \tag{27}$$

An entirely analogous approach to the problem of beam loading compensation can be used in the case of standing-wave structures. Figure 12(b) illustrates symbolically how the standing-wave section "fills vertically" (shaded area) instead of longitudinally, and how the bunch train can be injected at time $t_P - t_B$.

One final comment that must be made about using bunch trains is that their advantage probably diminishes as one goes up in RF frequency: indeed, since the filling time t_F decreases as $\omega^{-3/2}$, a point is eventually reached where t_B can no longer be decreased accordingly because the individual bunches in the train get too close to each other, and begin to interact unfavorably in the accelerator, or disrupt their adjacent counterparts in the final focus. It has been suggested that a solution to the disruption problem is to skew the e^+ and e^- trajectories in the final focus at a small angle so that e^- bunch (n) does not disrupt e^+ bunch $(n+1)$ before the latter interacts with e^- bunch $(n+1)$. However, an interbunch spacing of a few meters or nanoseconds is perhaps a lower limit.

3.7 Examples of Linacs

In this final section, we will now examine the consequences of the major points discussed in this paper by looking at some examples of 1 TeV (c.m.) linacs. To simplify the discussion, all designs will be of the constant gradient type and use a τ of 0.57.

Column (0) in Table 2 gives the main parameters of the SLC. The power out of each klystron (P_k = 156 MW) is the equivalent peak power after the SLED cavities. Each klystron feeds four 3.05 m sections. The factor of 2 in the

efficiencies $\eta_{ST\to B}$ and $\eta_{AC\to B}$ refers to the fact that in the SLC, the e^+ and e^- bunches are accelerated by the same linac. Note that all the efficiencies are quite low.

Columns (1) through (5) in Table 2 all represent designs using the beam parameters listed in the righthand-side column of Table 1, namely $N = 2.5 \times 10^{10} e^{\pm}$, $b = 10$, $f = 120$ pps, $\epsilon_n = 10^{-5} m_0 c$-m, $\sigma_z = 1$ mm and $2P_B = 4.8$ MW.

Column (1) illustrates what happens if we simply scale the SLC by a factor of 10 in length but hold the other RF parameters constant. To the extent that it resembles the present SLAC linac, this design roughly balances the costs due to length with those due to power. Its main disadvantage is its total length ($\sim$ 60 km) which does not even include the beam switchyards and final foci. Clearly, such a machine is impractical, difficult to align and control, and uses too much power.

The example in Column (2) also uses SLAC-type sections but assumes operating them at a six-times higher gradient (123 MV/m), chosen to be somewhat below the 150 MV/m experimental breakdown point. We thus obtain two much shorter linacs with a smaller number of RF sources and sections. However, as expected, each RF feed point requires a huge amount of peak power (1404 MW) as well as average power (140 kW). The peak power can probably not be reached with practical single tubes nor does it seem easily attainable through power multiplication. Furthermore, the AC power for this example is much too high and would even be higher, had we not assumed the improved $\eta_{AC\to ST}$ efficiency of 30%. Finally, this design makes poor use of the energy stored.

Column (3) again uses SLAC-type sections but only at a gradient three-times higher than the SLC (61.5 MV/m). This is probably the most "reasonable" design in that it requires the least number of technological jumps. When we think of the SLC, remembering that it uses the SLAC linac twice, it is really 6 km long (plus the length of the arcs and final foci). The example in Column (3) is only three times as long ($\sim$ 17 km) for ten times the energy. The number

Table 2. Linac Related Parameters

	SLC	1 TeV (c.m.) ($2.5 \times 10^{10} e^{\pm}$/ bunch)				
	($5 \times 10^{10} e^{\pm}$/bunch)	(All conditions as in Table 1, Column 3)				
	(0)	(1)	(2)	(3)	(4)	(5)
$E_{c.m.}$ (GeV)	2×50	2×500, $b = 10$ bunches				
G (MV/m)	20.5	20.5	123	61.5	102.5	143.5
F (GHz)	2.856	2.856	2.856	2.856	5.712	8.568
λ (mm)	105	105	105	105	52.5	35
L (km)	2.9	29×2	4.2×2	8.4×2	5×2	5×2
N_k (power sources)	240	2400×2	1380×2	2754×2	4630×2	8475×2
N_s (sections)	960	9600×2	1380×2	2754×2	4630×2	8475×2
P_k (MW) equiv.	156	156	1404	351	244	212
τ	0.57	0.57	0.57	0.57	0.57	0.57
t_F (μsec)	0.83	0.83	0.83	0.83	0.29	0.16
ℓ (m)	3.05	3.05	3.05	3.05	1.08	0.59
P_0/m (MW/m)	11.5	11.5	414	103.5	203	323.4
$P_0 t_F/m$ (J/m)	9.55	9.55	344	86	59	51.8
W_{ST} (J/m)	5.64	5.64	203	50.75	35.2	30.5
f (pps)	180	120	120	120	120	120
$\eta_{AC \to ST}$	8.8%	8.8%	30%	30%	30%	30%
$P_{AC,TOTAL}$ (MW)	33.6	446	682	341	141	122
$\eta_{ST \to B}$	2.8% ($\times 2$)	13%	2.3%	4.7%	11.2%	13%
$\eta_{AC \to B}$	0.25% ($\times 2$)	1.1%	0.7%	1.4%	3.4%	3.9%

of klystrons and sections is high (5500), but such a number is going to be a fact of life with any long machine. The main question that will have to be answered for this example and for the two subsequent ones is: how do we reach the peak powers in the 200 to 400 MW range with the $\eta_{AC\rightarrow RF}$ efficiency of 50% that leads to the $\eta_{AC\rightarrow ST}$ of 30% postulated to make the machine energy-viable? Note that, referring back to Fig. 8, an $\eta_{AC\rightarrow RF}$ of 50% means that one has to come up with a power source that is at least 70% efficient because the high voltage modulator and waveguide losses will add inefficiencies of their own. Will it be easier to attain the 1 μsec pulses of 350 MW peak power (every 3 meters!) with an extremely high voltage and medium perveance tube, or with a medium voltage and very high perveance tube, or with, say a more modest tube giving 100 MW for 4 μsec pulses which is then power-boosted with a ($\times 4$), i.e., two-stage compressor-multiplier? Modulator efficiency is always decreased by rise and fall times, and from that point of view, longer pulses are more efficient. Extremely high voltages (above 500 kV) require different circuits from the ones used in conventional line-type modulators and pulse transformers. For a given output power, lower voltages dictate higher tube perveances ($i/V^{3/2} > 2$) which traditionally have yielded lower efficiency. Finally, if we settle for a tube in the 100 MW output range, what will be the efficiency and cost of energy compression-multiplication to boost it to 400 MW? Will we need superconducting delay lines to make energy compression-multiplication viable?

Columns (4) and (5) show examples where we have gone respectively to twice (5712 MHz) and three-times (8568 MHz) the SLAC frequency. In these designs we have also pushed the gradients by factors of 5 and 7 respectively above the SLC, so as to satisfy roughly the criterion that the beams should extract 10% of the stored RF energy. As we see, the numbers of power sources, accelerator sections and necessary waveguide feeds increase rapidly but the peak powers, filling times, average powers, section lengths and stored energies all come down. However, with the gradients we have assumed (to keep overall length and total number of sources and/or energy compression-multiplication stages within reason), and in

keeping with the scaling rules of Eqs. (22), the value of P_0/m is still going up. Furthermore, if the "difficulty" in producing high power for a given tube-type really scales as $\omega^{2.5}$ (i.e., the power drops as $\omega^{-2.5}$), then an increasing burden will be placed on energy compression-multiplication, and here we do not yet know the pitfalls of this new technology. Another problem that must be faced in going to higher frequencies is the $\sim \omega^2$ and $\sim \omega^3$ scaling law of longitudinal and transverse wakefields.

Concerning the longitudinal wakes, one will hopefully always be able to find theoretical bunch shapes for any given design that will cancel the energy spread within a bunch, but probably at the cost of adjusting σ_z to values shorter than the 1 mm chosen in Table 1. However, assuming that there are damping rings and compressors capable of producing these shapes, once we reduce σ_z we decrease the value of the disruption parameter D: then, unless we accordingly increase the number of particles or decrease the invariant emittance below $10^{-5} m_0 c$-m, the luminosity will suffer. In Column (5) we have kept a σ_z of 1 mm but have placed the bunch far ahead of crest, at the loss of some efficiency.

Concerning the transverse wakefields, three fundamental questions come up. The first is whether it will be possible to improve upon the mechanical tolerances of the SLC by one or two orders of magnitude, and at what cost. The second has to do with the costs of controlling the wakefields by brute focusing strength and/or Landau damping. The third one has to do with the use of multibunches and the memory of the transverse wakefields from bunch to bunch. As the frequency rises to three times the SLAC frequency and the filling time falls to 160 nsec, one is forced to reduce the bunch spacing if one wants to fit, say ten bunches at the end of one filling time, or increase the RF pulse length accordingly, which then increases the overall power demand. What is the bunch-to-bunch memory? How many RF cycles apart must we keep them to avoid cumulative emittance growth within the train?

These are only some of the problems that must be studied before we can

comfortably move up in frequency, basically to save power. It may turn out that an actual machine can be optimized by dividing it into two segments, one at lower frequency at the beginning to minimize the effect of wakefields, the other one at a higher harmonic frequency, to save length and power.

4. Conclusions

In this paper, we have concerned ourselves with some of the crucial issues which are raised when one wants to use conventional technology to design a 1 TeV (c.m.) $e^{\pm}$ linear collider with a luminosity of 2×10^{32} cm^{-2} sec^{-1}. To study these issues, we have separated somewhat artificially the beam-related problems from the linac-related problems. In the case of the beam-related problems, we have been rather conservative and have not tried to depart too much from the SLC specifications, except for the rather large number (10) of bunches per pulse. In the case of the linac-related problems, we have raised many of the issues that are generally considered in linac design, and have explored what happens as one goes to gradients and frequencies higher than the SLC, in an attempt to decrease overall length and power consumption. The examples and the discussion in Section 3.7 give a fairly good idea of the RF and other problems that one has to confront as one goes to higher energies, quite independently of beam characteristics. Many of these problems will become even more severe as one tries to go beyond the 1 TeV (c.m.) range.

For lack of either urgency, competence or time, we have not discussed the following problems:

- Low emittance e^- injector design
- e^+ source design
- Damping rings or alternate schemes
- Timing tolerances having to do with synchronization over very long distances

- Use of RF superconductivity
- Energy recovery from RF to DC
- Mass production of modular elements.

Developments in the last two or three of these areas could have a major impact on how the "conventional technology" as defined in the introduction evolves and succeeds (or fails) to live up to the challenges of $e^{\pm}$ linear collider requirements.

Also, because of all the technical uncertainties, we have not in this paper gone into explicit discussions of financial costs, although they have been implicit in many of our considerations and trade-offs. One very general reference point to keep in mind is that if we had to build the SLC from the ground up today, using two 3 km-long SLAC linacs, it would cost at least $1 billion. Thus, not too surprisingly, a machine with ten times the center-of-mass energy could cost $10 billion if the same technology were used and no economies of scale were to be achieved. Such cost, however, would be prohibitive. Clearly, to survive and stay on the famous Livingston curve, one must either improve existing technology or invent a new one.

Acknowledgements

The author wishes to thank Perry B. Wilson from whose Ref. 2 he borrowed many ideas, and Roger H. Miller and Wang Juwen for useful discussions.

References

1. B. Richter (SLAC) in the Proceedings of this Summer Institute, July 1985; P.B. Wilson (SLAC) in the Proceedings of this Summer Institute, July 1985; R.D. Ruth (SLAC) in the Proceedings of this Summer Institute, July 1985; R. Palmer (SLAC/Brookhaven) in the Proceedings of this Summer Institute, July 1985.

2. P. B. Wilson, "Linear Accelerators for TeV Colliders," Invited paper presented at the 2nd International Workshop on Laser Acceleration of Particles, Los Angeles, CA, January 7-18, 1985, SLAC-PUB-3674.

3. B. Richter, "Very High Energy Colliders," Invited paper presented at the 1985 Particle Accelerator Conference, Vancouver, B.C., Canada, May 13-16, 1985, SLAC-PUB-3669.

4. G. A. Loew and R. Talman, "Elementary Principles of Linear Accelerators," Proceedings of the 1982 Summer School on High Energy Particle Accelerators, Stanford Linear Accelerator Center, Stanford, CA, August 1982, SLAC-PUB-3221.

5. R. B. Neal, "Accelerator Parameters for an e^+e^- Super Linear Collider," SLAC/AP-7, September 1983.

6. J. W. Wang and G. A. Loew, "Measurements of Ultimate Accelerating Gradients in the SLAC Disk-Loaded Structure," IEEE Trans. Nucl. Sci. **NS-32**, No. 5, October 1985, SLAC-PUB-3597.

7. P. B. Wilson, "High Energy Electron Linacs: Application to Storage Ring RF Systems and Linear Colliders," Proceedings of the 1981 Summer School on High Energy Particle Accelerators, Fermi National Accelerator Laboratory, Batavia, Illinois, July 1981, SLAC-PUB-2884.

8. G. A. Loew, M. A. Allen, R. L. Cassel, N. R. Dean, G. T. Konrad, R. F. Koontz and J. V. Lebacqz, "The SLC Energy Upgrade Program at SLAC," IEEE Trans. Nucl. Sci. **NS-32**, No. 5, October 1985, SLAC-PUB-3609.

9. T. G. Lee, *et al.*, "The Design and Performance of a 150 MW Klystron at S-Band," SLAC-PUB-3619, March 1985.

10. E. L. Garwin, W. B. Herrmannsfeldt, C. Sinclair, J. N. Weaver, J. J. Welch and P. B. Wilson, "An Experimental Program to Build a Multimegawatt Lasertron for Super Linear Colliders," IEEE Trans. Nucl. Sci. **NS-32**, No. 5, October 1985, SLAC-PUB-3650.

11. V. L. Granatstein, P. Vitello, K. R. Chu, K. Ko, P. E. Latham, W. Lawson, C. D. Striffler, and A. Drobot, "Design of Gyrotron Amplifiers for Driving 1 TeV e^-e^+ Linear Colliders," IEEE Trans. Nucl. Sci. **NS-32**, No. 5, October 1985.

12. D. B. Hopkins and R. W. Kuenning, "The Two-Beam Accelerator: Structure Studies and 35 GHz Experiments," IEEE Trans. Nucl. Sci. **NS-32**, No. 5, October 1985.

13. Z. D. Farkas, *et al.*, "SLED: A Method of Doubling SLAC's Energy," Proc. of the IXth Int. Conf. on High Energy Accelerators, May 1974, p. 576.

14. Z. D. Farkas, *et al.*, "Binary Power Multiplier," SLAC-PUB-3694 to be published.

15. "SLAC Linear Collider Conceptual Design Report," SLAC Report No. 229, June 1980.

16. R. Stiening, "An Introduction to the Accelerator Physics of Linear Colliders," Proceedings of the 1982 Summer School on High Energy Particle Accelerators, Stanford Linear Accelerator Center, Stanford, CA, August 1982.

17. A. W. Chao, B. Richter and C. Y. Yao, "Beam Emittance Growth Caused by Transverse Deflecting Fields in a Linear Accelerator," Nuclear Instruments and Methods **178** (1980), SLAC-PUB-2498.

18. G. A. Loew and J. W. Wang, "Minimizing the Energy Spread Within a Single Bunch by Shaping Its Charge Distribution," IEEE Trans Nucl. Sci. **NS-32**, No. 5, October 1985, SLAC-PUB-3598.

19. K.L.F. Bane, "Landau Damping in the SLAC Linac," Contributed paper to the 1985 Particle Accelerator Conference, Vancouver, B.C., May 13-16, 1985, SLAC-PUB-3670.